Ultrasonics Sonochemistry 18 (2011) 608–616

Contents lists available at ScienceDirect

Ultrasonics Sonochemistry

journal homepage: www.elsevier.com/locate/ultsonch

Kinetics of sono-photooxidative degradation of poly(alkyl methacrylate)s

R. Vinu, Giridhar Madras *

Department of Chemical Engineering, Indian Institute of Science, Bangalore 560012, India

ARTICLE INFO

Article history:
Received 7 July 2010
Received in revised form 2 September 2010
Accepted 9 September 2010
Available online 17 September 2010

Keywords:
Ultrasound
Ultraviolet
Sonochemical
Photochemical
Sonophotochemical
Poly(alkyl methacrylate)

ABSTRACT

The mechano-chemical degradation of poly(methyl methacrylate) (PMMA), poly(ethyl methacrylate) (PEMA) and poly(*n*-butyl methacrylate) (PBMA) using ultrasound (US), ultraviolet (UV) radiation and a photoinitiator (benzoin) has been investigated. The degradation of the polymers was monitored using the reduction in number average molecular weight (M_n) and polydispersity (PDI). A degradation mechanism that included the decomposition of the initiator, generation of polymer radicals by the hydrogen abstraction of initiator radicals, reversible chain transfer between stable polymer and polymer radicals was proposed. The mechanism assumed mid-point chain scission due to US and random scission due to UV radiation. A series of experiments with different initial M_n of the polymers were performed and the results indicated that, irrespective of the initial PDI, the PDI during the sono-photooxidative degradation evolved to a steady state value of 1.6 ± 0.05 for all the polymers. This steady state evolution of PDI was successfully predicted by the continuous distribution kinetics model. The rate coefficients of polymer scission due to US and UV exhibited a linear increase and decrease with the size of the alkyl group of the poly(alkyl methacrylate)s, respectively.

© 2010 Elsevier B.V. All rights reserved.

1. Introduction

Power ultrasound (20–100 kHz) is widely used to initiate, accelerate and change the reaction pathway of a number of aqueous and organic phase reactions [1]. The chemical effect of ultrasound (US) is due to the nucleation and growth of cavitation bubbles during the rarefaction cycle of the sound wave. The catastrophic collapse of these bubbles during the compression phase results in picosecond flashes of light, called sonoluminescence, and extreme local temperatures and pressures of 5000 K and 1000 atm [2]. These conditions provide sufficient energy for the formation of radicals, which initiate chemical reactions. This provides a possibility of reactions like the synthesis of nanostructured materials, heterogeneous catalysis [3] and polymer degradation [4]. The degradation of polymers by US results in the breakage of the polymer around the mid-point. The rupture of bonds is due to the intense shock wave that is radiated at the final stages of the collapse of a cavitating bubble [4,5]. This sets up velocity gradients between the solvent and the polymer chains, which causes maximum stress to be located at the center of mass of the polymer chain, thereby resulting in the scission around the mid-point. This mechanical mode of scission of polymers also results in the limiting chain length, as the stresses setup within the polymer of minimum size cannot exceed the bond strength [4]. Many studies [5–9] elucidate the effect of different physical parameters like temperature, vapor pressure, viscosity, polymer concentration, initial molecular weight, solution pH, solvents, dissolved gases and US intensity on the degradation of different polymers in solution.

Many mechanistic and phenomenological models have been proposed to describe the kinetics of polymer scission during ultrasonic treatment. Akyüz et al. [10] have compared several of the models published in the literature and conclude that the predictions of the Ovenall/Harrington/Madras, and the Giz and Tang models, which incorporate the initial rapid decrease of molecular weight followed by the slowing down of the molecular weight till the limiting molecular weight, agree well with the experimental data. However, following only the number average molecular weight (M_n) of the polymers during degradation does not provide a complete description of the degradation behavior. A more thorough description is the time evolution of molecular weight distribution (MWD) of the polymers during degradation, which can shed light on the mechanism of degradation. Madras and McCoy [11,12] have used the distribution kinetics approach to predict the time evolution of the MWD using the gamma distribution parameters. Their models predict the time evolution of polydispersity (PDI) to a steady state value of unity at long US exposure periods. Sivalingam et al. [13] have used a Lorentzian function as the breakage kernel to describe the distribution of polymer species around the mid-point. Their model captures the initial increase of PDI of a monodisperse sample, and the subsequent decrease to reach an asymptotic value of unity. The degradation kinetics based on viscometry has been used to determine the rate constants for degradation of water soluble polymers [14,15].

* Corresponding author. Tel.: +91 80 22932321; fax: +91 80 23601310.
E-mail address: giridhar@chemeng.iisc.ernet.in (G. Madras).

1350-4177/$ - see front matter © 2010 Elsevier B.V. All rights reserved.
doi:10.1016/j.ultsonch.2010.09.005

Another means by which chemical reactions can be coupled to US is by the use of an alternate source of energy like the ultraviolet (UV) radiation. UV exposure is a well recognized technique to degrade polymers and it is well known that the mode of scission is purely random [16,17]. The simultaneous ultrasonic and photolytic (sonophotolytic) reactions have gained immense interest in heterogeneous catalysis for the decontamination of aqueous organic pollutants like dyes [18] and phenolic compounds [19], in presence of nano-sized TiO_2. The sonophotocatalytic systems exhibit higher mineralization rates compared to the individual photocatalytic or sonocatalytic processes. However, the utilization of simultaneous US and UV to effect the degradation of polymers is a new concept, and only two studies [20,21] have explored the sonophotocatalytic degradation of chitosan [20] and water soluble polymers [21]. In our previous work on the sonophotocatalytic degradation of poly(ethylene oxide), poly(acrylic acid) and poly(vinyl pyrrolidone) using TiO_2 [21], a ternary chain scission model was found to describe the kinetics quite satisfactorily in terms of the time evolution of M_n and PDI. However, the mid-point scission induced by US was not considered, and the degradation was modeled using binary and ternary random scission in presence of UV and US. In this study, we attempt to incorporate both binary random scission and mid-point scission in the model.

Therefore, the aim of this study is to integrate the individual contributions of US and UV to the polymer scission to predict the time evolution of M_n and PDI for the degradation of a series of poly(alkyl methacrylate)s, viz., poly(methyl methacrylate) (PMMA), poly(ethyl methacrylate) (PEMA) and poly(*n*-butyl methacrylate) (PBMA). PMMA, a widely used thermoplastic, finds applications in glass replacements, intraocular lenses, fixing dentures, and in paints and lubricating fluids. Importantly, MMA is copolymerized with other methacrylates and acrylates to improve the impact strength, glass transition temperature, and thermal- and photostability. Hence, the mechano-chemical degradation of these polymers can be used to modify the properties of the end product and for the effective remediation of the waste plastics.

Therefore, in this work, we report the sono-photooxidative degradation of PMMA, PEMA and PBMA in presence of toluene as the solvent, and benzoin as the photoinitiator. A detailed degradation mechanism has been proposed and modeled using continuous distribution kinetics. The time evolution of M_n and PDI are discussed based on the mechanism of chain scission.

2. Experimental section

2.1. Materials and methods

The monomers, ethyl methacrylate (EMA) and butyl methacrylate (BMA), were procured from Sigma Aldrich, and methyl methacrylate (MMA) was purchased from Rolex Chemicals, India. MMA and BMA were washed initially with 5% caustic solution and then with water to remove the hydroquinone inhibitor. The initiators, azobisisobutyronitrile (AIBN, Sigma Aldrich) and benzoin (S.D. Fine Chemicals, India) were used as received. Tetrahydrofuran (THF) and toluene (Merck, India) were of HPLC grade.

All the poly(alkyl methacrylate)s, except PEMA1 (Sigma Aldrich) (see Table SI 1 in supplementary information), were synthesized by free radical bulk polymerization. Polymers of different M_n were synthesized by using different concentrations of AIBN ranging from 0.15 to 0.45 wt.% in 10 mL of the respective monomer solutions. The monomer and initiator solutions were polymerized at 60 °C under nitrogen atmosphere in a thermostated water bath. The synthesized polymers were precipitated twice in methanol for the removal of unreacted monomer and dried until constant weight was obtained. The M_n and PDI of the synthesized polymers are shown in Table SI 1 (see supplementary information).

2.2. Sonophotolytic reactor

All the degradation experiments were conducted in a sonophotolytic reactor. The polymer solution to be degraded was taken in a jacketed borosilicate glass container of 5.2 cm i.d., 7.6 cm o.d. and 10 cm height. The ultrasonic horn (Vibronics, India; frequency – 25 kHz) of 1″ dia. was dipped into the polymer solution such that the distance between the bottom of the container and the horn was 2 cm. This ensured that the polymer solution was continuously stirred using a magnetic stirrer and the experiments were repeatable. Stirring the reaction mixture helps in the dispersal of the cavitation bubbles throughout the reaction volume. The UV light source was 125 W high pressure mercury vapor lamp (HPML) placed inside a jacketed quartz tube of 4 cm i.d., 4.7 cm o.d. and 18 cm height. The distance between the UV light source and the reaction vessel was 1 cm. Cold water was circulated in the jacket of the container and in the annulus of the quartz tube to quench the heat generated, and to maintain the reaction temperature at 35 °C. The schematic of the sonophotolytic reactor is provided in Fig. SI 2 (see supplementary information). The actual power intensity of the US horn determined by a standard calorimetric technique [1], ranged from 1.2 to 2.7 W cm^{-2}. The power intensity was varied by adjusting the voltage input to the processor. The UV lamp radiated predominantly at 365 nm, and the intensity and photon flux calculated by *o*-nitrobenzaldehyde actinometry [22] were 10.5 μEinstein s^{-1} and 965 μW cm^{-2}, respectively. During the 7 h experiments, the change in the actual power intensity was less than 1% and the variation of the temperature of the solution was less than 0.1 °C.

2.3. Degradation experiments

All the sonolytic and sono-photooxidative degradation experiments were carried out in toluene as the solvent. The reasons for the choice of the solvent are discussed in the results and discussion section. The reaction volume was 100 mL and the US power intensity was fixed at 1.2 W cm^{-2}. The concentrations of the initiator and the polymer were 11.78 mmol L^{-1} (2.5 g L^{-1}) and $3.1 \pm 0.1 \times 10^{-6}$ mol L^{-1}, respectively. Aliquots of 0.5 mL were withdrawn at periodic intervals for the determination of M_n and PDI.

2.4. Analysis

The samples were analyzed for M_n and PDI in a gel permeation chromatograph (GPC). The GPC system consisted of a Waters 510 HPLC pump, Rheodyne 7725i injector (sample loop – 0.2 mL), three size exclusion columns (Waters HR-5E, HR-3 and HR-0.5, measuring 300 mm × 7.5 mm, maintained at 30 °C) and a differential refractometer (Waters 2410). The eluent, THF, was pumped at a flow rate of 1 mL min^{-1}. The columns were calibrated using eleven poly(styrene) narrow standards (Polymer Standards, USA, and TSK Standards, Japan) of molecular weight (MW) ranging from 500 to 3.8×10^6 g mol^{-1}. The calibration equation based on MW and retention time was used to convert the chromatogram to molecular weight distribution. The concentration of the initiator during UV + US exposure was determined by monitoring the reduction of peak height in the GPC chromatogram.

3. Mechanism of sono-photooxidative degradation

The proposed mechanism of sono-photooxidative degradation of poly(alkyl methacrylate)s is based on the experimental

observations, and the reactions are modeled using continuous distribution kinetics. This approach accounts for the size distribution of the polymer and polymer radicals, and hence the MW, x, of the polymer ($P(x)$)and the polymer radical ($R_{\bullet}(x)$) is treated as a continuous variable. Such models have been previously applied for the degradation of polymers using non-conventional sources of energy like US [8], UV [17] and microwave [23]. However, the model derived in this work is new for sono-photooxidative degradation of polymers.

3.1. Reversible initiation and termination

$$P(x) \xrightarrow{k_i} R^{\bullet}(x') + R^{\bullet}(x - x') \tag{A1}$$

$$R^{\bullet}(x') + R^{\bullet}(x - x') \xrightarrow{k_t} P(x') + P(x - x') \tag{A2}$$

This step signifies the formation of polymer radicals by the initiation of the stable polymer species (reaction (A1)) and the termination of the polymer radicals to form the stable polymer (reaction (A2)). As the predominant mode of termination of alkyl methacrylates is by disproportionation [24], we have ignored the termination reaction by combination. The above reactions, along with hydrogen abstraction and chain scission form the elementary steps of Rice-Herzfeld mechanism [25], proposed originally for the thermal cracking of organic compounds. The rate of initiation is very small due to the high activation energy (80–90 kcal mol^{-1}) of this step [26]. Therefore, compared to the frequency of the chain scission reactions (Section 3.6) whose activation energy usually lies in the range 30–40 kcal mol^{-1} [27], the initiation reaction can be ignored. Moreover, owing to the high reactivity and low concentration of the radicals, the rate of termination reaction is also small. The above two limiting conditions are known as the long chain approximation (LCA). It is important to note, however, that these reactions are essential for the degradation to start and terminate. Smagala and McCoy [28] have compared the polymer and radical concentration profiles obtained by the full numerical solution with the analytical solution, and conclude that the predictions of the analytical solution with LCA agrees well with the numerical solution in the initial time range of less than 10 to 20 h of reaction time, for the analysis of experimental data. Also, the PDI profiles predicted by the numerical and analytical solution techniques were in good agreement with each other. Therefore, we have ignored the contribution of the rate coefficients, k_i and k_t to the overall reaction rate.

3.2. Hydrogen abstraction

$$P(x) + R^{\bullet}(x') \rightleftharpoons S^{\bullet}(x + x') \rightleftharpoons P(x') + R^{\bullet}(x) \tag{B1}$$

$$P(x) \underset{k_H}{\overset{k_h}{\rightleftarrows}} R^{\bullet}(x) \tag{B2}$$

This reaction represents the chain transfer of polymer to polymer radical and vice versa, through the formation of a radical adduct species, S. This unstable intermediate species undergoes β-scission to yield the polymer and radical species with the chains interchanged. The bimolecular reaction (B1) can be reduced to the form represented by reaction (B2) by the application of pseudo steady state approximation on the intermediate species [28]. This is known as the hydrogen abstraction reaction, as a polymer radical is formed by the abstraction of a proton from the stable polymer, and the addition of a proton to the polymer radical yields a stable polymer species. The hydrogen abstraction reaction can also occur within the chain, i.e., intramolecular, resulting in the formation of a radical around the mid-point or at random position within the chain. The representation in reaction (B2) does not differentiate between a chain end and an inter chain radical. Chiantore et al. [29] have shown by UV/Vis and FT-IR spectroscopy that inter chain polymer radicals are indeed formed when poly(ethyl methacrylate) is exposed to UV radiation. These radicals serve as scission centers leading to the formation of a stable polymer species and a fragment radical, according to reaction (F). The chain length independent rate coefficients are given by k_H and k_h [27,28,30].

3.3. Photodecomposition of the initiator

$$C_6H_5CH(OH)COC_6H_5 \xrightarrow{h\nu} C_6H_5C^{\bullet}H - OH + C_6H_5C^{\bullet} = 0 \tag{C1}$$

$$I_2 \xrightarrow{k_d} I^{\bullet}_{\alpha} + I^{\bullet}_{\beta} \tag{C2}$$

Benzoin is one of the most common photoinitiators and upon excitation with UV radiation, benzoin undergoes α-cleavage to form two radical species, viz., hydroxy benzyl radical ($I^{\bullet}_{\alpha}$) and benzoyl radical ($I^{\bullet}_{\beta}$) [31]. The first-order rate constant of this induced decomposition is given by k_d.

3.4. Hydrogen abstraction by the initiator radicals

$$P(x) + I^{\bullet} \xrightarrow{k_i} R^{\bullet}(x) + I - H \tag{D}$$

Hageman and Overeem [32] have established by NMR and mass spectroscopy that both the radicals ($I^{\bullet}_{\alpha}$) and ($I^{\bullet}_{\beta}$) are involved in reactions like hydrogen abstraction, dimerization and solvent attack to form benzaldehyde, benzil, benzophenone and pinacol derivatives. The abstraction of a proton from the polymer species to form a polymer radical is the major reaction of the benzoyl radical and the minor reaction for the hydroxy benzyl radical. However, in the proposed mechanism, we do not distinguish the contribution of either of the radicals in the hydrogen abstraction reaction, and hence the initiator radical is denoted as $I^{\bullet}$, with rate coefficient k_1. The major and minor side products (I–H) of this reaction are benzaldehyde and benzyl alcohol, respectively.

3.5. Radical capping by the initiator

$$R^{\bullet}(x) + I_2 \xrightarrow{k_2} P(x) + I^{\bullet} \tag{E}$$

This reaction represents the formation of stable polymer species from the polymer radical by the interaction with the initiator. In this reaction, the initiator radical acts to cap off the polymer radical, thereby forming the stable polymer. Daraboina and Madras [8] have recently reported that common thermal initiators like benzoyl peroxide, AIBN and dicumyl peroxide undergo this reaction to stabilize the degradation of poly(alkyl methacrylate)s by US. However, in our experiments with benzoin as the initiator for the US degradation of PEMA1, it was observed that the concentration of the initiator remained constant even after long hours (>7 h) of US exposure, and the M_n and PDI profiles were comparable with that observed for sonolysis. This shows that benzoin initiates the polymer radicals only by the UV pathway (reaction (D)) and it has no interaction with US. To further verify this, the concentration of benzoin was monitored when only benzoin was sonolyzed. The concentration did not change, indicating that benzoin does not cleave under US exposure. Furthermore, our initial simulations with this reaction revealed that the rate coefficient k_2 has a negligible effect on the overall concentration profiles of the polymer. Hence, we have ignored the contribution of reaction (E) in the derivation of rate equations.

3.6. Radical chain scission

$$\begin{aligned} &-CH_2 - \dot{C}(X) - CH_2 - C(CH_3)(COOR) - \rightarrow \\ &\quad -CH_2 - C(X) = CH_2 + \dot{C}(CH_3)(COOR) - \end{aligned} \tag{F1}$$

where X is $-CH_3$ or $-COOR$

$$R^{\cdot}(x) \xrightarrow{k_b(x)} P(x') + R^{\cdot}(x - x') \quad \text{(F2)}$$

The final reaction is the breakage or scission of the polymer radical of MW x to yield stable polymer species of MW x', and a polymer radical fragment of MW x-x'. The polymer radical which undergoes scission is one where the radical is within the chain, and not at the chain end (reaction (F1)). Such radicals are usually formed in poly(alkyl methacrylate)s by the abstraction of a methyl radical or ester radical in presence of UV radiation [29,33]. We have included the mid-point scission due to US ($x' = x/2$) and the random scission due to UV radiation. Hence, the rate coefficient, $\kappa_b(x)$, for this reaction is given by $\kappa_b(x) = \kappa_{b,UV}(x) + \kappa_{b,US}(x)$. The random scission rate coefficient due to UV contribution, which has a linear dependence on MW, is given by $\kappa_{b,UV}(x) = k_{b,UV}x$ [12]. The rate coefficient for the mid-point chain scission due to US is given by $\kappa_{b,US}(x) = k_{b,US}(x - x_L)$ [6,11], where x_L is the limiting MW. This is consistent with our experimental results that at long time periods, M_n of the poly(alkyl methacrylate)s approaches a limiting value when degraded with US + UV + benzoin. Moreover, the absence of any low MW compounds like monomers or oligomers in the GPC chromatogram, confirmed the absence of depolymerization reaction and shows that the scission is primarily due to mid-point and random chain scission mechanisms.

3.7. Rate equations

A detailed derivation of the rate equations is given in Appendix A (see SI 3 in supplementary information). The rate equations for the initiator and the polymer species involved in reaction mechanism (A) to (F) are given by (see SI 3 in supplementary information)

$$-\frac{d[I_2]}{dt} = k_d[I_2] \quad (1)$$

$$\frac{dp^{(n)}}{dt} = -k_h p^{(n)} + k_H r^{(n)} - k_d[I_2]\frac{p^{(n)}}{p^{(0)}} + \frac{k_{b,UV}}{n+1}r^{(n+1)} + \frac{k_{b,US}}{2^n}\left(r^{(n+1)} - r^{(n)}x_L\right) \quad (2)$$

The solution of Eq. (1) is given by $[I_2] = [I_2]_0 \exp(-k_d t)$, where $[I_2]_0$ is the initial initiator concentration. The rate coefficient k_d was determined experimentally by degrading the initiator of different concentrations in toluene in presence of UV + US. By this, k_d was determined to be $10^{-4}\ s^{-1}$. The decomposition rate of the initiator was also monitored in presence of the polymers and it was found that the above value of k_d was not significantly affected.

In order to predict the time evolution of M_n and PDI, given by $p_0^{(1)}/p^{(0)}$, and $p^{(2)}p^{(0)}/p_0^{(1)^2}$, respectively. Eq. (2) was solved numerically for $n = 0$ and 2, with the initial conditions $p^{(0)}(t=0) = p_0^{(0)} = p_0^{(1)}/M_{n,t=0}$ and $p^{(2)}(t=0) = p_0^{(2)} = PDI_{t=0}p_0^{(1)^2}/p_0^{(0)}$ by fitting the experimental data of polymer molar concentration ($p^{(0)}$) and polymer second moment ($p^{(2)}$). The expressions for $r^{(0)}$, $r^{(1)}$, $r^{(2)}$ and $r^{(3)}$ are given in Appendix A (see SI 3 in supplementary information).

4. Results and discussion

4.1. Initial experiments

Fig. 1(a) shows the experimental profiles of M_n during the degradation of PMMA1 in toluene under different conditions. It is clear that the combinative system of US + UV + benzoin results in the higher initial rate of degradation compared to the US + UV system without benzoin. This occurs till most of the initiator is consumed in the formation of initiator radicals that abstract hydrogen from the stable polymer to form polymer radicals, according to reaction (D). However at long time periods, the profiles are nearly the same and a limiting M_n is attained. The degradation of PMMA1 with only US proceeds at a lower rate compared to the US + UV systems, and the time evolution of M_n to the limiting MW is also slower. Finally, the UV + benzoin results in the slowest degradation of PMMA1 compared to all the systems. This shows that US is the primary contributor for the degradation of the polymer and the effect of UV + initiator is only to accelerate the degradation in the initial time period. The PDI profiles in Fig. 1(b) suggest that, for the photooxidative degradation, the PDI approaches a limiting value of 2, in agreement with the pure random scission of polymers [12]. The PDI profile for the sonolytic degradation shows a continuous decrease suggesting that it tends to the limiting value of 1. Moreover, as all the synthesized polymers were polydisperse (PDI > 2.4), an initial increase in PDI was not observed. Interestingly, the PDI for the sono-photolytic degradation with and without the initiator exhibits a steady value of 1.6 ± 0.05 at long time periods, indicating that the effect of coupling of UV radiation to US is to increase the PDI (>1), characteristic of the random scission of the polymer. We will show in the forthcoming sections that this is the limiting value of PDI for the degradation of all the poly(alkyl methacrylate)s.

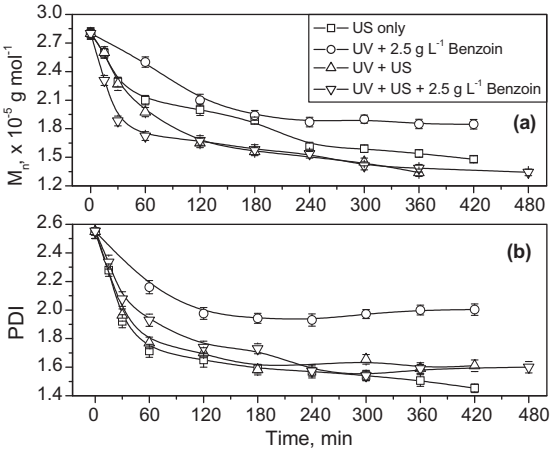

Fig. 1. Experimental time evolution profiles of (a) M_n and (b) PDI for PMMA1 under various conditions of US and UV irradiation.

4.2. Reaction conditions

Based on the initial observations, sonolytic and sono-photooxidative degradation of a series of poly(alkyl methacrylate)s were performed. PMMA, PEMA and PBMA of three different initial M_n and PDI (Table SI 1 in supplementary information) were degraded in toluene as the solvent. It is well known that solvents with higher vapor pressure reduce the intensity of shock wave radiated during the collapse of the bubbles, due to the cushioning effect of the vapor inside the cavitation bubble. Hence, the US degradation of polymers in different solvents follows the order: 1,2-dichlorobenzene (DCB) > xylene ≈ chlorobenzene > toluene > ethyl acetate > benzene [8,34]. However, we have used toluene as the solvent in all our experiments. The reasons can be attributed to the following: firstly, in the initial sono-photooxidative experiments with DCB, yellowing of the polymer solution was observed within 15 min of irradiation. In order to confirm if the yellowing of the solution is due to the reactions of the ester side group of the methacrylates or due to the solvent itself, pure DCB was exposed to UV radiation. It was observed that the darkening of the solution was more pronounced. This can be primarily attributed to the formation of intermediates like substituted chlorophenolic compounds [35]. These intermediates, apart from affecting the kinetics of the degradation

of the polymer, might filter the incident UV radiation from reaching the polymer chains. This was also observed for chlorobenzene, but at longer time periods. Therefore toluene was chosen as the solvent for all the reactions. Furthermore, the low viscosity of toluene compared to the other solvents might facilitate the mobility of the polymer radicals in undergoing scission by UV radiation. Thus, our choice of toluene as the "optimum solvent" for the combined US + UV degradation is validated.

From Table SI 1 (see supplementary information), it is clear that for each poly(alkyl methacrylate), the initial M_n and PDI are different, and in order to have a fair comparison of the degradability of the polymers by the combined action of US + UV + initiator, the mass concentration has to be varied. This is because, the effect of UV + benzoin is to accelerate the degradation by the abstraction of protons from the polymer species, and hence, the oxidizer to abstractable hydrogen ratio is a crucial factor that determines the degradation of the polymers. Thus, for a constant molar concentration of the initiator, the polymer molar concentration has to be the same for all the polymers. Therefore, the mass concentration of the polymers was varied based on the initial M_n to conserve this quantity. We have used a polymer molar concentration of $3.1 \pm 0.1 \times 10^{-6}$ mol L^{-1}, which corresponds to a mass concentration of 0.1–0.4% w/v for the different polymers. This concentration range is in the dilute solution limit, and so no significant variation in the rate of degradation would occur due to the effect of US [36]. Moreover, it is well known that polymers with higher M_n, degrade at higher rates, while polymer solutions of high concentration degrade at lower rates in presence of US [4,7]. This also supports our argument that the polymer mass concentration should be different for polymers of different initial M_n to compare the degradation rates. Therefore, the experimental conditions we have chosen correspond to the maximum degradation rates attainable with both UV and US.

4.3. Solution of the rate equations

The ordinary differential rate equation (2) for $n = 0$ and 2, were solved for three different initial conditions, corresponding to three different initial M_n for PMMA and PEMA at 2.5 g L^{-1} benzoin, and five different initial conditions for PBMA (three different initial M_n and three different initial initiator concentrations – 2.5, 5 and 8 g L^{-1}). The equations were numerically solved using Runge Kutta 4th order formula in Matlab, by assuming realistic initial values for the rate coefficients k_h, k_H, $k_{b,UV}$ and $k_{b,US}$, from the literature [8,30,33]. The output of this function was fed to the non-linear curve fitting module 'lsqcurvefit', which works on the basis of interior reflective Newton algorithm. The updated values of the rate coefficients were used to solve the rate equations in the next iteration, till the convergence criterion is met. The convergence was monitored by a residual, which is defined as the sum of the squares of the deviations of the experimental and model values. The iteration was stopped when the residual was minimum and invariant. For the sonolytic degradation of poly(alkyl methacrylate)s, the initiator concentration and the scission rate coefficient due to UV ($k_{b,UV}$) were set to zero, and the simulation was carried out for three different initial M_n of PMMA, PEMA and PBMA. Table 1 shows the rate coefficients for different polymer systems, and the error associated with these rate coefficients was less than 5%.

4.4. Model correlations

Figs. 2–4 depict the experimental and model correlated time evolution profiles of $p^{(0)}$, $p^{(2)}$, M_n and PDI for the sono-photooxidative degradation of PMMA2, PEMA2 and PBMA2 with 2.5 g L^{-1} benzoin. It is clear that the model correlates the exact time evolution of $p^{(0)}$ and $p^{(2)}$, and thereby M_n and PDI for all the polymers. The time evolution of M_n and PDI to the limiting values was also predicted by the model. The limiting molecular weights for PMMA, PEMA and PBMA were 1.3×10^5, 1.35×10^5 and 1.5×10^5 g mol^{-1}, respectively, and the limiting PDI was 1.6 ± 0.05 for all the poly(alkyl methacrylates). This shows that the expression for the second radical moment ($r^{(2)}$) given by Eq. (A.10) (see SI 3 Appendix A in supplementary information), and hence the assumption that the PDI of the polymer radicals is equal to that of the polymer species, is indeed valid over the entire range of degradation reaction. Moreover, the skewness of the distribution is a useful quantity to express the third moment ($r^{(3)}$) in terms of the lower order moments. We have also cross-checked this with the PDI profiles obtained, when $r^{(3)}$, computed by the interpolative closure technique, was expressed as [37,38]

$$r^{(3)} = \frac{2r^{(2)^2}}{r^{(1)}} - \frac{r^{(2)}r^{(1)}}{r^{(0)}} \tag{3}$$

We found that the PDI profiles were the same for both the expressions for $r^{(3)}$.

Table 1
Rate coefficients for the sono-photooxidative and sonolytic degradation of poly(alkyl methacrylate)s.

Rate coefficients	PMMA	PEMA	PBMA
UV + US + Benzoin			
k_h, s^{-1}	0.025 ± 0.0015	0.08 ± 0.004	0.10 ± 0.005
k_H, s^{-1}	13.0 ± 0.70	17.5 ± 0.90	27.5 ± 1.40
$k_{b,UV}$, × 10^{-8} mol g^{-1} s^{-1}	2.4 ± 0.12	2.0 ± 0.12	1.6 ± 0.08
$k_{b,US}$, × 10^{-8} mol g^{-1} s^{-1}	3.2 ± 0.15	4.2 ± 0.20	5.5 ± 0.28
US only			
k_h, s^{-1}	0.13 ± 0.006	0.18 ± 0.01	0.20 ± 0.01
k_H, s^{-1}	4.0 ± 0.20	7.0 ± 0.40	11.0 ± 0.50
$k_{b,USonly}$, × 10^{-8} mol g^{-1} s^{-1}	1.4 ± 0.08	1.8 ± 0.08	2.5 ± 0.12

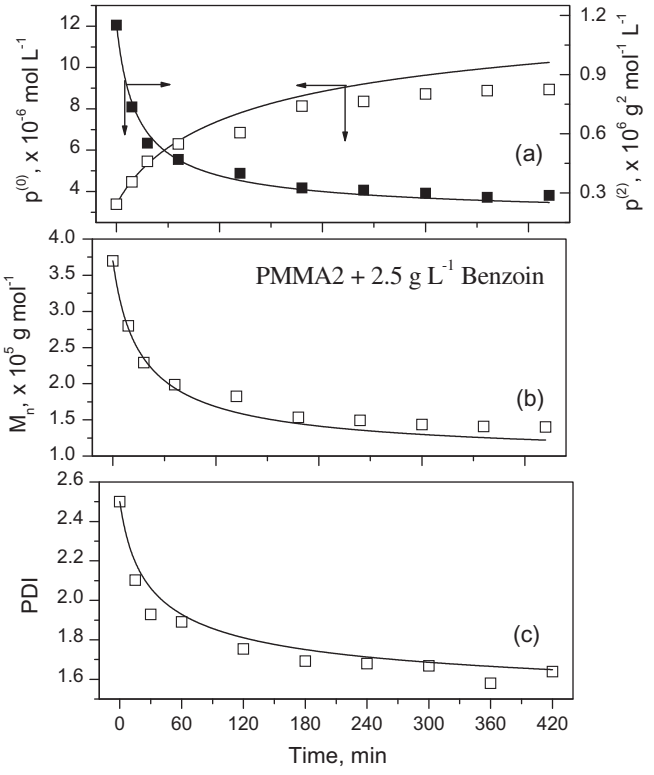

Fig. 2. Experimental and model fitted time evolution profiles of $p^{(0)}$, $p^{(2)}$, M_n and PDI for the sono-photooxidative degradation of PMMA2 in presence of 2.5 g L^{-1} of benzoin. Lines are model fits.

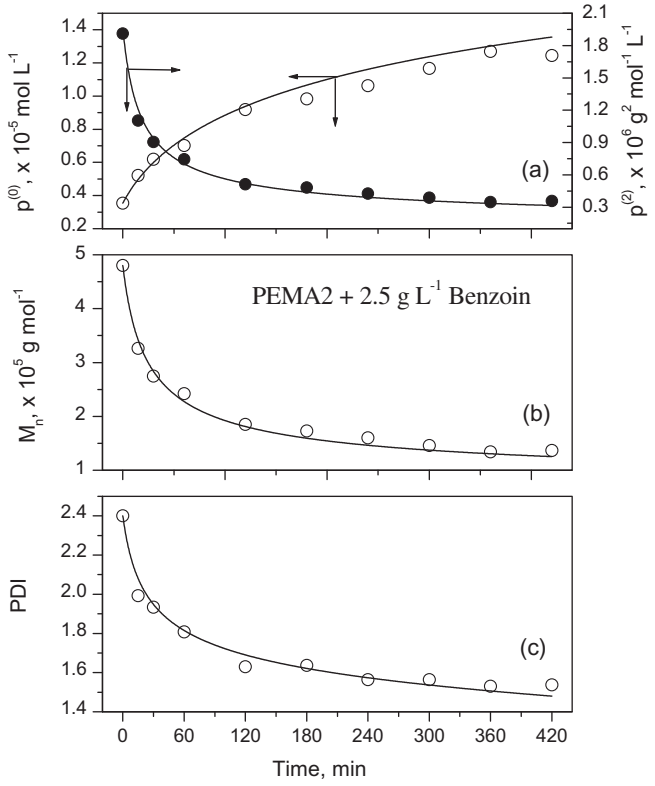

Fig. 3. Experimental and model fitted time evolution profiles of $p^{(0)}$, $p^{(2)}$, M_n and PDI for the sono-photooxidative degradation of PEMA2 in presence of 2.5 g L^{-1} of benzoin. Lines are model fits.

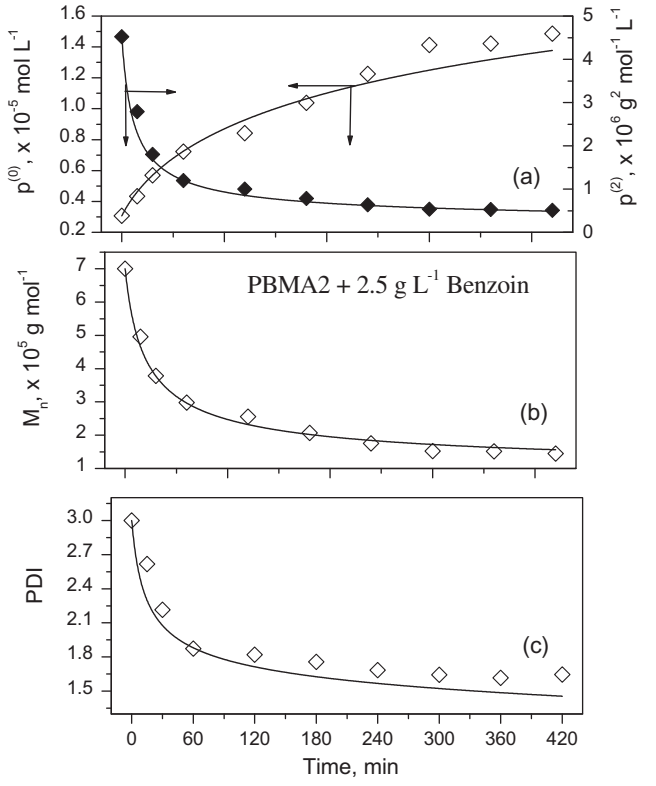

Fig. 4. Experimental and model fitted time evolution profiles of $p^{(0)}$, $p^{(2)}$, M_n and PDI for the sono-photooxidative degradation of PBMA2 in presence of 2.5 g L^{-1} of benzoin. Lines are model fits.

Fig. 5 shows the time evolution profiles of M_n and PDI for PBMA3 when degraded with three different initial concentrations of the initiator. The model predicts the M_n profiles quite well over the entire time period, while the PDI profiles are predicted well only in the initial time periods. At long time periods (5–7 h), the model slightly under predicts the PDI. However, this is only slightly higher than the experimental standard deviation of 0.05. Importantly, the model captures the saturation of the PDI at long time periods, which is characteristic of sono-photooxidative degradation. Hence, it is clear that higher concentrations of the initiator accelerate the initial degradation of the polymer by the formation of more polymer radicals, which can undergo scission by both US and UV. Nevertheless, the limiting M_n is not affected by the initiator, as it depends only on the solvent properties and the US intensity. The model predictions show that the M_n profiles tend to reach a limiting value at long time periods.

Fig. SI 4 (see supplementary information) shows the time evolution profiles of $p^{(0)}$, $p^{(2)}$, M_n and PDI for the sonolytic degradation of PBMA3. As the rate of degradation of the polymer is lesser with only US irradiation, the scission rate coefficient due to US ($k_{b,US}$) is able to capture the profiles satisfactorily without the contribution from UV. This shows that the scission rate coefficient due to UV ($k_{b,UV}$), is not an artifact to describe the kinetics of sono-photooxidative degradation, but an intrinsic parameter that accounts for the random scission of the polymer chains. In fact, the exclusion of $k_{b,UV}$ in the model Eq. (2) to describe the sono-photooxidative degradation resulted in poor predictions, especially in the initial time when the effect of UV + oxidizer is more pronounced. Further, from Fig. SI 5 (see supplementary information), the predictions of the model for the sonolytic degradation of PMMA2, PEMA2 and PBMA2 are in agreement with the experimental data. The model, apart from predicting the limiting M_n, also predicts the evolution of

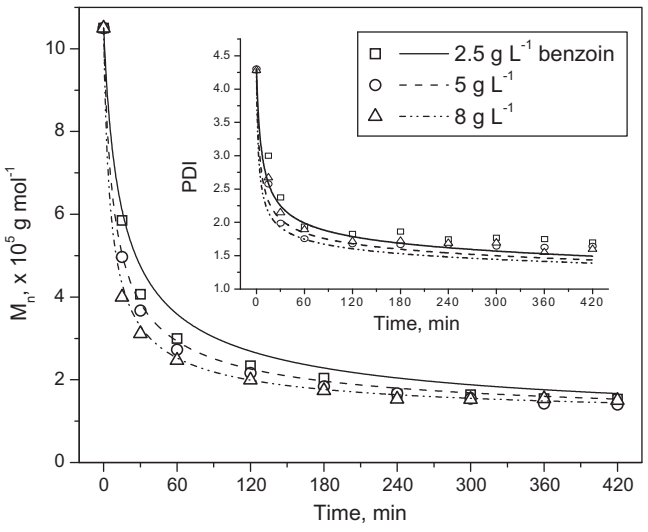

Fig. 5. Effect of initial initiator concentration on the time evolution profiles of M_n and PDI (inset) for PBMA3. Lines are model fits.

PDI tending towards a limiting value of 1 at longer exposure hours (>7 h).

Fig. 6 and Fig. SI 6 (see supplementary information) compares the M_n and PDI profiles during the sono-photooxidative and sonolytic degradation of PMMA1, PEMA1 and PBMA1, and PMMA3 and PEMA3, respectively. The accelerating effect of UV + initiator is very clear from the high initial rate of decrease of M_n. It can also be observed that, for the sonolytic degradation of PMMA1 and PEMA1 (Fig. 6(a) and 6(b)), the evolution to the limiting M_n is much

slower compared to PBMA1 (Fig. 6(c)), PMMA3 and PEMA3 (Fig. SI 6 in supplementary information). This suggests that polymers with low M_n are degraded at lower rates compared to those with high M_n. This is consistent with the observation that long chain polymers offer more resistance to flow, thereby accumulating greater shear forces resulting in more frequent breakage. From the inset figures, it can be concluded that, for all the polymers, the sono-photooxidative degradation results in a limiting value of PDI of 1.6 ± 0.05, while the sonolytic degradation results in a continuous decrease of PDI towards unity.

4.5. Validation of rate coefficients

The order of the model fitted hydrogen abstraction rate coefficients, k_H and k_h, in Table 1, for both sono-photooxidative and sonolytic degradation agree well with the previously reported values of Madras and McCoy [30], for the degradation of poly(styrene) in presence of tetralin (a hydrogen donor). It can be observed that both k_H and k_h, increase with an increase in the alkyl side group of the poly(alkyl methacrylate)s. This means that the rate of formation of polymer radicals by hydrogen abstraction, and the formation of stable polymer species by proton addition are higher for alkyl methacrylates with bulky side groups. The important factor that determines the ease of formation of the radicals is the mobility of the polymer chains. It is well proven that the order of glass transition of the poly(alkyl methacrylate)s follows: PMMA > PEMA > PBMA [16]. Hence, with increase in size of the side chain, the free volume increases, thereby resulting in an increase of chain mobility. Hence, our model fitted values of the hydrogen abstraction rate coefficients reflect the exact trends. The order of the scission rate coefficients, $k_{b,US}$ and $k_{b,UV}$, also match with the previous studies of the photo- and sonolytic degradation of poly(alkyl methacrylate)s [8,33].

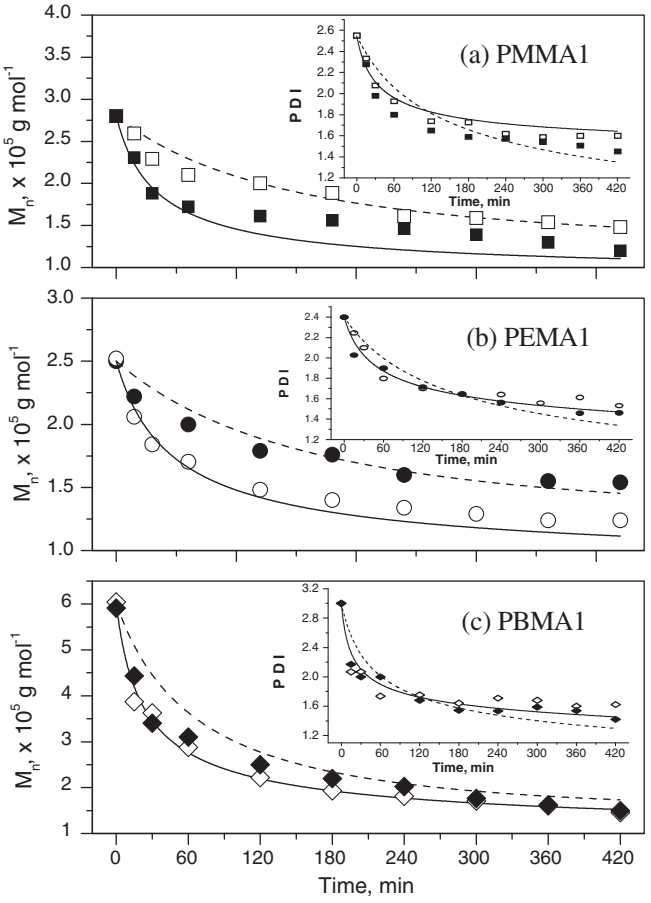

Fig. 6. Experimental and model fitted time evolution profiles of M_n and PDI (inset) for the sono-photooxidative and sonolytic degradation of (a) PMMA1 (b) PEMA1 and (c) PBMA1. [Legend: Open symbols/solid line – UV + US + 2.5 g L^{-1} benzoin; Filled symbols/dashed line – US only].

The rate coefficients, $k_{b,US}$ and $k_{b,UV}$, signify the US contribution to polymer scission in the presence of UV radiation, and the UV contribution to polymer scission in the presence of US, respectively. In our reaction mechanism, the radicals are formed by both UV and US, i.e., by the hydrogen abstraction reactions due to UV and US (reactions B1 and B2), and due to the hydrogen abstraction of the initiator radicals by UV (reaction D). The mechanism does not incorporate the radicals formed by UV and US, separately. Hence, the proposed mechanism is indeed non-additive in terms of the rate coefficients.

In fact, the rate coefficient, $k_{b,UV}$, is an order of magnitude higher compared to that previously observed for the photocatalytic degradation of PMMA with TiO_2. This shows the accelerating effect due to the combination of US + UV + initiator in the degradation. The rate coefficient, $k_{b,US}$ (O(10^{-8})) is two orders of magnitude higher than the rate coefficient k_1 (=$k_b k_h/k_H$) reported for the US degradation of polymers [8]. However, the incorporation of the hydrogen abstraction rate coefficients with $k_{b,US}$ would suggest that the order is nearly the same. It can also be observed that $k_{b,US}$, for the sono-photooxidative degradation is 50% higher than the sonolytic degradation for all the poly(alkyl methacrylate)s. This shows that the US contribution to the degradation of the polymer is enhanced by coupling with UV radiation. Therefore, the above discussion confirms the observation previously made for the sonophotocatalytic degradation of water soluble polymers [21], that the effect of US + UV on the degradation of the polymers is not just an additive effect of the rate coefficients of the individual processes, but a net synergism due to the interaction of both the competing processes.

The order of the scission rate coefficients reported in this work also matches well with the rate coefficients of the individual processes. Among the poly(alkyl methacrylate)s, the main chain scission due to UV follows the order: PMMA > PEMA > PBMA [16], while the order is the reversed for US degradation [8]. This variation can also be observed in the present work for $k_{b,UV}$ and $k_{b,US}$ for the sono-photooxidative degradation, where these rate coefficients exhibit a linear variation with the length of the alkyl side chain of the alkyl methacrylates (Fig. 7).

4.6. Effect of US and UV intensity

Interestingly, the limiting PDI for all the poly(alkyl methacrylate)s tends to 1.6 ± 0.05, irrespective of the initial M_n and the initial PDI of the polymers. This value lies in between the limiting values of 1 and 2, observed for the degradation of the polymer with only US and UV radiation, respectively. The fact that this is invariant with the initial M_n and PDI suggests that, the effect of UV + initiator and US on the degradation of the polymer is such that UV + initiator accelerates the degradation of the polymer in the initial period, and once most of the initiator is depleted, UV only acts to break the shorter polymer chains, while US exhibits a dominating effect in the scission of the longer chains. This combined action results in the PDI to evolve to a value between 1 and 2. The invariant nature of the limiting PDI for all the poly(alkyl methacrylate)s is suggestive of the fact that the scission occurs mostly in the main chain of the polymer and ester side groups are not involved. If UV radiation were to affect the side chains, then other oxidation products like aldehydes and ketones would be formed, which might result in different limiting PDI for each of the polymers. This is because PBMA has bulky butyl group, whose products of oxidation will have higher size compared to the oxidation products of PEMA and PMMA. This would result in a higher limiting PDI for PBMA compared to PEMA and PMMA.

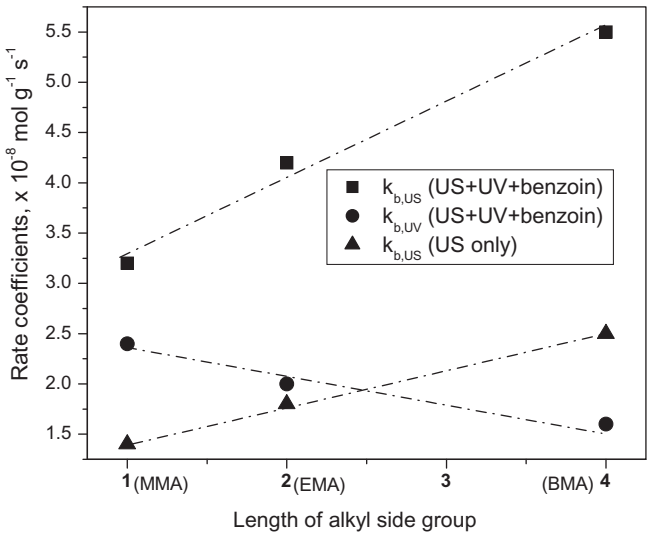

Fig. 7. Variation of the scission rate coefficients with the length of the alkyl side group of the poly(alkyl methacrylate)s.

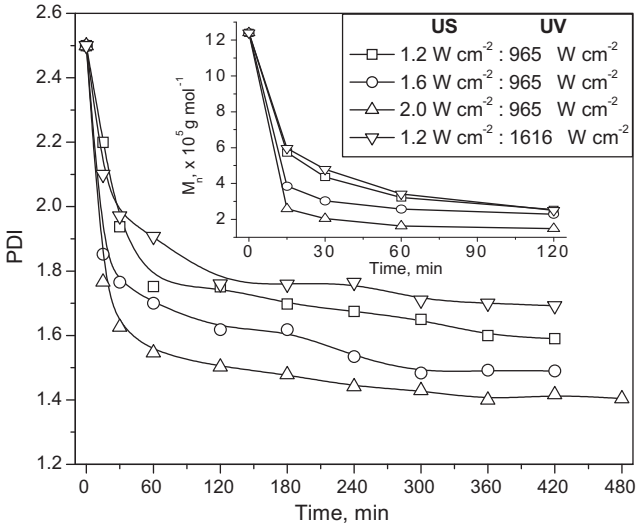

Fig. 8. Effect of US and UV intensity on the time evolution of M_n (inset) and PDI for the sono-photooxidative degradation of PMMA3 with 2.5 g L^{-1} benzoin.

As US plays a significant role in reducing the polymer PDI towards unity owing to its mechanical nature of scission, the factors that affect cavitation should also have an impact on the limiting PDI reached with the US + UV system. Hence, we have conducted the sono-photooxidative degradation of PMMA3 with 2.5 g L^{-1} benzoin, at three different US intensities, viz., 1.2, 1.6 and 2.0 W cm^{-2}. The result in Fig. 8 shows that the steady state PDI for different US intensities at a constant UV intensity of 965 μW cm^{-2} follows the order: 1.6 ± 0.05 (1.2 W cm^{-2}) > 1.5 ± 0.03 (1.6 W cm^{-2}) > 1.4 ± 0.04 (2.0 W cm^{-2}). This is also accompanied by a reduction of limiting M_n, which follows the same order. Price and Smith [5] have also observed a reduction in the limiting M_n and PDI with increasing US intensity for the degradation of poly(styrene). This is because the US intensity is proportional to the square of the acoustic pressure amplitude and increases the maximum radius of the cavitation bubbles during collapse. This leads to higher shear forces and, therefore, a lower value of limiting M_n and PDI is attained.

Similarly, by increasing the intensity of UV radiation it should be possible to decrease the limiting M_n and increase the PDI, as more number of shorter chains are susceptible to degradation at high UV intensities. To verify this, we have conducted an experiment with UV intensity of 1616 μW cm^{-2} (400 W HPML) and US intensity of 1.2 W cm^{-2}. The steady state evolution of PDI (Fig. 8) shows that the limiting PDI indeed increases to 1.7 ± 0.04, compared to that of 1.6 ± 0.05 with UV intensity of 965 μW cm^{-2}. The M_n profiles in the initial time period for both these conditions were nearly the same, while the limiting M_n was lower for the high UV intensity system. These suggest that, by tweaking the intensity of US and UV radiation, the PDI of the polymers can be tailored between 1 and 2. This opens up a new possibility of mechano-chemical reactions by coupling UV radiation with US to simultaneously degrade high polymers and modify the end properties (M_n and PDI) of the degraded polymer by simply altering the reaction conditions. Currently, it is not clear if the value of limiting PDI we have obtained is applicable for a wide class of polymers or is it restricted only to poly(alkyl methacrylate)s. For a thorough understanding of the process, our future studies would involve the effect of different operational parameters like UV intensity, US intensity, solvent characteristics and temperature on the final properties of various polymers during sono-photooxidative degradation.

5. Conclusions

In this study, we have evaluated the sono-photooxidative degradation of PMMA, PEMA and PBMA with benzoin as the photoinitiator, and toluene as the solvent. The polymers of varying initial M_n and PDI were synthesized and subjected to degradation. The time evolution profiles of M_n during the degradation suggested that the order of degradation among the different systems followed: US + UV + initiator > US + UV > US only > UV + initiator. The PDI profiles suggested that the sono-photooxidative degradation results in a limiting PDI of 1.6 ± 0.05 for all the poly(alkyl methacrylate)s, which is in between the limiting values of 1 and 2 for the US and UV degradation, respectively. An interesting aspect of the limiting PDI of the sono-photooxidative system is that, the final PDI varies between 1 and 2. The final PDI is 1 and 2 when the degradation occurs due to mid-point scission alone and UV alone, respectively. We show that by carefully selecting the reaction conditions (like UV and US intensity), the final MW and PDI of the poly(alkyl methacrylates) can be tuned. A comprehensive mechanism of degradation was proposed based on the accelerating effect of the initiator in the formation of polymer radicals by hydrogen abstraction, and the mid-point and random chain scission of the polymers induced by US and UV radiation, respectively. A continuous distribution kinetics model was used for correlating the degradation of the polymers. The model predicted time evolution profiles of M_n and PDI of the polymers during degradation were in good agreement with the experimental data, and all the salient features of the degradation were captured by the model. The scission rate coefficient due to US and UV exhibited a linear increase and decrease with the size of alkyl side chain of the poly(alkyl methacrylate)s, respectively. The possibility of altering the PDI of the degraded polymer by varying the US and UV intensity has been examined.

Acknowledgments

The corresponding author thanks the department of science and technology for financial support and the Swarnajayanthi fellowship.

Appendix A. Supplementary data

Supplementary data associated with this article can be found, in the online version, at doi:10.1016/j.ultsonch.2010.09.005.

References

[1] L.H. Thompson, L.K. Doraiswamy, Sonochemistry: science and engineering, Ind. Eng. Chem. Res. 38 (1999) 1215–1249.
[2] K.S. Suslick, D. Flannigan, Inside a collapsing bubble: sonoluminescence and the conditions during cavitation, Annu. Rev. Phys. Chem. 59 (2008) 659–683.
[3] K.S. Suslick, G.J. Price, Applications of ultrasound to materials chemistry, Annu. Rev. Mater. Sci. 29 (1999) 296–326.
[4] G.J. Price, The use of ultrasound for the controlled degradation of polymer solutions, in: T.J. Mason (Ed.), Advances in Sonochemistry, vol. 1, JAI press, Cambridge, 1990, p. 231.
[5] G.J. Price, P.F. Smith, Ultrasonic degradation of polymer solutions: 2. The effect of temperature, ultrasound intensity and dissolved gases on polystyrene in toluene, Polymer 34 (1993) 4111–4117.
[6] S.P. Vijayalakshmi, G. Madras, Effect of initial molecular weight and solvents on the ultrasonic degradation of poly(ethylene oxide), Polym. Degrad. Stab. 90 (2005) 116–122.
[7] S.P. Vijayalakshmi, G. Madras, Effects of the pH, concentration, and solvents on the ultrasonic degradation of poly(vinyl alcohol), J. Appl. Polym. Sci. 100 (2006) 4888–4892.
[8] N. Daraboina, G. Madras, Kinetics of ultrasonic degradation of poly(alkyl methacrylates), Ultrason. Sonochem. 16 (2009) 273–279.
[9] A. Akyüz, H. Catalgil-Giz, A.T. Giz, Effect of solvent characteristics on the ultrasonic degradation of poly(vinylpyrrolidone) studied by on-line monitoring, Macromol. Chem. Phys. 210 (2009) 1331–1338.
[10] A. Akyüz, H. Catalgil-Giz, A.T. Giz, Kinetics of ultrasonic polymer degradation: Comparison of theoretical models with on-line data, Macromol. Chem. Phys. 209 (2008) 801–809.
[11] G. Madras, B.J. McCoy, Molecular-weight distribution kinetics for ultrasonic reactions of polymers, AIChE J. 47 (2001) 2341–2348.
[12] G. Madras, B.J. McCoy, Numerical and similarity solutions for reversible population balance equations with size-dependent rates, J. Colloid Interface Sci. 246 (2002) 356–365.
[13] G. Sivalingam, N. Agarwal, G. Madras, Distributed midpoint chain scission in ultrasonic degradation of polymers, AIChE J. 50 (2004) 2258–2265.
[14] M.T. Taghizadeh, A. Mehrdad, Calculation of the rate constant for the ultrasonic degradation of aqueous solutions of polyvinyl alcohol by viscometry, Ultrason. Sonochem. 10 (2003) 309–313.
[15] M.T. Taghizadeh, A. Bahadori, Degradation kinetics of poly (vinyl-pyrrolidone) under ultrasonic irradiation, J. Polym. Res. 16 (2009) 545–554.
[16] H. Kaczmarek, A. Kamińska, A. van Herk, Photooxidative degradation of poly(alkyl methacrylate)s, Eur. Polym. J. 36 (2000) 767–777.
[17] A. Marimuthu, G. Madras, Photocatalytic oxidative degradation of poly(alkyl acrylates) with nano TiO_2, Ind. Eng. Chem. Res. 47 (2008) 2182–2190.
[18] R. Vinu, G. Madras, Kinetics of sonophotocatalytic degradation of anionic dyes with nano-TiO_2, Environ. Sci. Technol. 43 (2009) 473–479.
[19] R.A. Torres, J.I. Nieto, E. Combet, C. Pétrier, C. Pulgarin, Influence of TiO_2 concentration on the synergistic effect between photocatalysis and high-frequency ultrasound for organic pollutant mineralization in water, Appl. Catal. B: Environ. 80 (2008) 168–175.
[20] M.T. Taghizadeh, R. Abdollahi, Sonolytic, sonocatalytic and sonophotocatalytic degradation of chitosan in the presence of TiO_2 nanoparticles, Ultrason. Sonochem. 18 (2011) 149–157.
[21] T. Aarthi, M.S. Shaama, G. Madras, Degradation of water soluble polymers under combined ultrasonic and ultraviolet radiation, Ind. Eng. Chem. Res. 46 (2007) 6204–6210.
[22] K.L. Willett, R.A. Hites, Chemical actinometry; Using *o*-nitrobenzaldehyde actinometry to measure light intensity in photochemical experiments, J. Chem. Ed. 77 (2000) 900–902.
[23] A. Marimuthu, G. Madras, Continuous distribution kinetics for microwave-assisted oxidative degradation of poly(alkyl methacrylates), AIChE J. 54 (2008) 2164–2173.
[24] G. Moad, D.H. Solomon, The chemistry of Radical Polymerization, 2nd ed., Elsevier, Oxford, UK, 2006.
[25] F.G. Helfferich, Kinetics of Multistep Reactions, Elsevier, Amsterdam, 2004.
[26] W.J. Sterling, B.J. McCoy, Distribution kinetics of thermolytic macromolecular reactions, AIChE J. 47 (2001) 2289–2303.
[27] Y. Kodera, B.J. McCoy, Distribution kinetics of radical mechanisms: reversible polymer decomposition, AIChE J. 43 (1997) 3205–3214.
[28] T.G. Smagala, B.J. McCoy, Mechanisms and approximations in macromolecular reactions: reversible initiation, chain scission, and hydrogen abstraction, Ind. Eng. Chem. Res. 42 (2003) 2461–2469.
[29] O. Chiantore, L. Trossarelli, M. Lazzari, Photooxidative degradation of acrylic and methacrylic polymers, Polymer 41 (2000) 1657–1668.
[30] G. Madras, B.J. McCoy, Effect of hydrogen donors on polymer degradation, Catal. Today 40 (1998) 321–332.
[31] F.D. Lewis, R.T. Lauterbach, H.-G. Heine, W. Hartmann, H. Rudolph, Photochemical α cleavage of benzoin derivatives. Polar transition states for free-radical formation, J. Am. Chem. Soc. 97 (1975) 1519–1525.
[32] H.J. Hageman, T. Overeem, Photoinitiators and photoinitiation, 4: trapping of primary radicals from photoinitiators by 2, 2, 6, 6-tetramethylpiperidinoxyl, Makromol. Chem., Rapid Commun. 2 (1981) 719–724.
[33] R. Vinu, G. Madras, Photocatalytic degradation of methyl methacrylate copolymers, Polym. Degrad. Stab. 93 (2008) 1440–1449.
[34] J.P. Mahalik, G. Madras, Effect of alkyl group substituents, temperature, and solvents on the ultrasonic degradation of poly(*n*-alkyl acrylates), Ind. Eng. Chem. Res. 44 (2005) 6572–6577.
[35] R. Andreozzi, M. Canterino, R. Marotta, Fe(III) homogeneous photocatalysis for the removal of 1, 2-dichlorobenzene in aqueous solution by means UV lamp and solar light, Water Res. 40 (2006) 3785–3792.
[36] G.J. Price, P.F. Smith, Ultrasonic degradation of polymer solutions–III. The effect of changing solvent and solution concentration, Eur. Polym. J. 29 (1993) 419–424.
[37] T.M. Kruse, H.-W. Wong, L.J. Broadbelt, Modeling the evolution of the full polystyrene molecular weight distribution during polystyrene pyrolysis, Ind. Eng. Chem. Res. 42 (2003) 2722–2735.
[38] M. Evans, N. Hastings, B. Peacock, Statistical Distributions, John Wiley, Singapore, 2000.